Robust Methodology for Low-Frequency Noise Power Analyses in Advanced MOS Transistors

Léopold Van Brandt
ICTEAM, Université catholique de Louvain, Louvain-la-Neuve, Belgium, leopold.vanbrandt@uclouvain.be

Babak Kazemi Esfeh Valeria Kilchytska Denis Flandre

***Abstract*—We present a new methodology to discriminate random telegraph noise (RTN) and flicker (1/f) noise components from set-up noise. We illustrate it for a strong RTN case ($\Delta I_{\mathrm{D}}/I_{\mathrm{D}} \approx 30\,\%$) measured on a $26\,\mathrm{nm}$ gate length nMOS transistor. The approach is based on high-accuracy time-domain measurements. An iterative Schmitt trigger-like algorithm was developed to properly identify and model the RTN and 1/f noise. Statistical analysis allows to assess the accuracy of the extraction. The power spectral densities (PSD) of the different noise models accurately match the frequency measurements.**

I. Introduction

The minimal gate length transistors, favoured for the design of digital integrated circuits, are very sensitive to all types of variability. Among them, the low-frequency noise (LFN), a time-dependent variability, has become a major concern for the design of ultra-low power (ULP) circuits, operating at downscaled supply voltage and hence at lower *signal-to-noise ratio* (SNR).

One usual approach to characterize and model low-frequency noise consists in measuring the noise power spectral density (PSD) [1]–[3]. While requiring few post-processing, this treats both random telegraph noise (RTN) and flicker ($1/f$) noise sources together as "LFN". Separation of RTN and $1/f$ noise was performed in [4], but the technique relied on rather complicated switched bias conditions. The physical properties of RTN and related traps are also widely studied from drain current time trace measurements [5], [6].

However the very different relative impacts of RTN and $1/f$ noise components are rarely quantified and discussed with regards to circuit applications, in terms of noise powers. This, in particular, relies on the rigorous realization, processing and modelling of measurements of relevance for circuit design, i.e. on minimal gate length transistors, appropriate bias conditions, at ultra-low power, with a very high accuracy in terms of time step and frequency bandwidth. Our present work addresses this problem.

II. Measurement Details

We have measured multiple short-channel nMOS transistors using a Keysight ALFNA noise analyzer [7]. One transistor with $W = 1\,\mu\mathrm{m}$ and $L = 26\,\mathrm{nm}$, biased at fixed drain voltage $V_{\mathrm{DS}} = 0.3\,\mathrm{V}$ (in saturation) and normalized drain current $I_{\mathrm{D}}/(W/L) = 10^{-8}\,\mathrm{A}$ (corresponding to the weak inversion), was selected to illustrate our methodology. 5M samples per measurement were recorded with a time step $\mathrm{d}t = 80\,\mathrm{ns}$. A representative portion of the measured zero-mean drain current noise

$$i_{\mathrm{d}}(t) = i_{\mathrm{D}}(t) - I_{\mathrm{D}} \tag{1}$$

trace is shown in Fig. 1a.

The RTN is seen to be very strong, as $\Delta I_{\mathrm{D}}/I_{\mathrm{D}} \approx 30\,\%$, and was chosen in purpose to illustrate that, even in this case, the $1/f$ noise can be properly distinguished and modelled. The time step has been selected according to the observed RTN time constants and required frequency bandwidth at circuit level. Here, the RTN time constants are notably short and hence requires a much faster sampling rate than usually used [6].

III. Processing Methodology and Results

A. RTN and $1/f$ Noise Extraction

Toward accurate compact modelling of the different intrinsic noise sources, careful separation of the individual noise components is required. A robust algorithm is needed to discriminate RTN from other noise sources. Ours is based on a Schmitt trigger-like estimation of the two RTN levels. The extraction procedure starts from a peak detection algorithm applied to the histogram of $i_{\mathrm{d}}(t)$ and is repeated in an iterative way, in order to capture the shorter duration RTN events. The obtained RTN trace $i_{\mathrm{d,RTN}}(t)$ is illustrated in Fig. 1b. Our signal processing also eliminates part of the set-up noise.

The residual noise, is computed as

$$i_{\mathrm{d,flicker}}(t) = i_{\mathrm{d}}(t) - i_{\mathrm{d,RTN}}(t)\,. \tag{2}$$

It is denoted by $i_{\mathrm{d,flicker}}(t)$ as it will be shown to be dominated by the $1/f$ component. We observe in Fig. 1c the presence of few glitches or short-wing shapes which can be attributed to remaining parasitics and artifacts of the measurement and extraction procedure, yet to be fully eliminated. However they do not alter our coming noise power analyses.

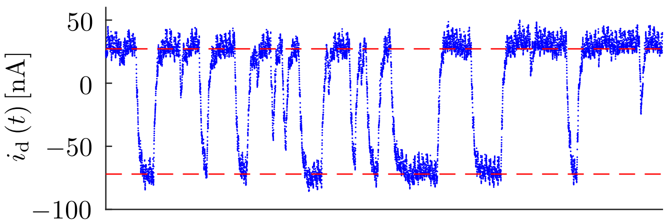

(a)

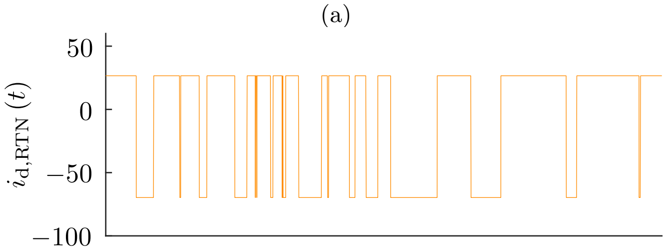

(b)

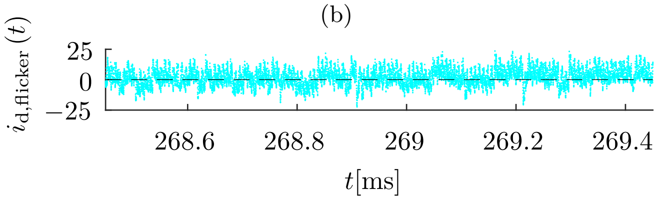

(c)

Fig. 1: (a) Measured drain current noise $i_\mathrm{d}(t) = i_\mathrm{D}(t) - I_\mathrm{D}$ trace, (b) extracted RTN and (c) residual noise.

B. Statistics

1) RTN time constants: Given $i_{\mathrm{d,RTN}}(t)$ of Fig. 1b, the *capture* and *emission time constants* are readily computed. The experimental distributions of these two time constants are available in Fig. 2a and 2b, respectively.

It can be shown from purely mathematical consideration that the time constants are exponentially distributed around their respective means, $\overline{\tau}_\mathrm{c}$ and $\overline{\tau}_\mathrm{e}$ [5], [8]:

$$f_{\mathcal{T}}(\tau) = \frac{1}{\overline{\tau}} \exp\left(-\frac{\tau}{\overline{\tau}}\right). \tag{3}$$

The means can be estimated empirically: $\overline{\tau}_\mathrm{c} \approx 22\,\mu\mathrm{s}$ and $\overline{\tau}_\mathrm{e} \approx 9.5\,\mu\mathrm{s}$. The theoretical distributions are also represented in Fig. 2a and 2b. There is a fair agreement between experience and theory for both time-constant types, which supports the accuracy of our RTN extraction.

2) Histogram of $i_\mathrm{d}(t)$: The histogram of the drain current noise, after the removal of instrumentation noise, is presented in Fig. 3. Two Gaussians are centered on each RTN level. The distance between the two peaks yields the RTN amplitude, $\Delta I_\mathrm{D} \approx 100\,\mathrm{nA}$. The ratio between the peak occurrences, here about 2.3, is consistent with the calculated $\overline{\tau}_\mathrm{c}/\overline{\tau}_\mathrm{e}$ ratio.

C. Power Spectral Densities and Noise Powers

1) PSD and the $1/f$ Nature of the Residual Noise: To obtain the second-order statistics of the residual noise, and confirm that this noise can be unambiguously related to the intrinsic $1/f$ noise of the transistor, its PSD

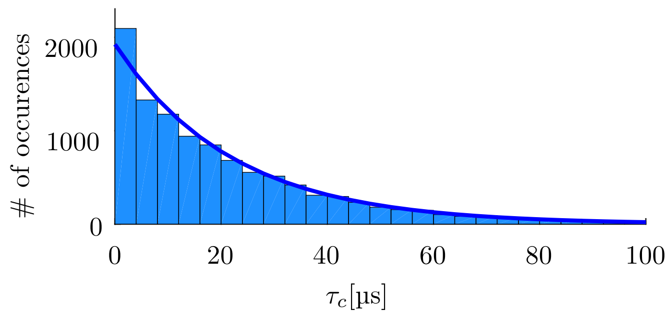

(a)

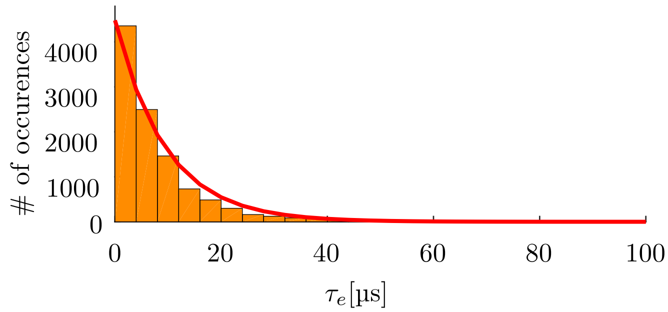

(b)

Fig. 2: Time-constant distributions: (a) $\mathcal{T}_c$ and (b) $\mathcal{T}_e$. Solid lines represent the theoretical distributions (3).

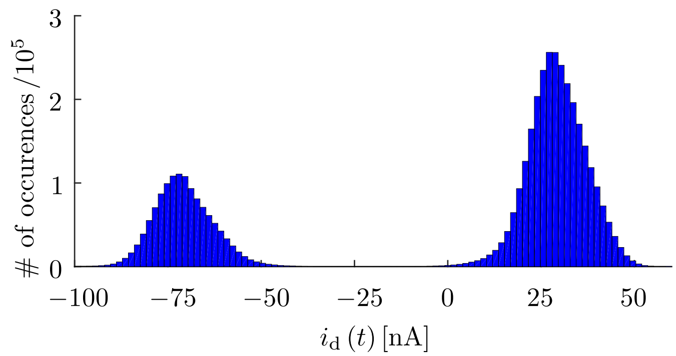

Fig. 3: Histogram of $i_\mathrm{d}(t)$.

$\widehat{S}_{i_{\mathrm{d,flicker}}}(f)$ is estimated from the realization $i_{\mathrm{d,flicker}}(t)$, using a spectral estimation method [9] (Fig. 4). Remarkably, we observe a very clean $1/f$ behaviour in the $\left[10^2\,\mathrm{Hz}, 10^3\,\mathrm{Hz}\right]$ band. The deviation for frequencies beyond 10^3 Hz can be attributed to the set-up and processing related parasitics still observed in Fig. 1c. A mathematical flicker noise model

$$S_{i_{\mathrm{d,flicker}}}(f) = \frac{S_{1\,\mathrm{Hz}}}{f^a} \tag{4}$$

is fairly fitted to the estimated PSD (Fig. 4), yielding $S_{1\,\mathrm{Hz}} \approx 8 \times 10^{-18}\,\mathrm{A}^2/\mathrm{Hz}$ and $a \approx 0.95$.

To assess the accuracy of our estimated $1/f$ PSD, we compare it with an accurate measurement performed with the same equipment. As shown in Fig. 4, our model closely

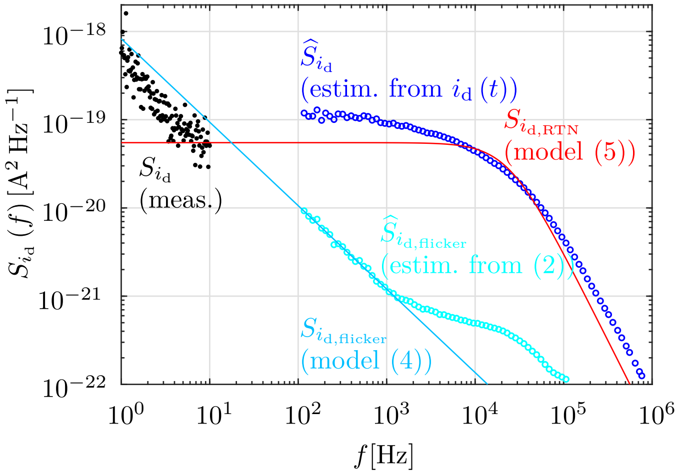

Fig. 4: Power spectral densities.

Noise powers	$\sigma^2_{i_d}\,[\mathrm{A}^2]$	$\sigma^2_{i_{d,RTN}}\,[\mathrm{A}^2]$	$\sigma^2_{i_{d,flicker}}\,[\mathrm{A}^2]$
Time domain (7)	2.165×10^{-15}	1.949×10^{-15}	6.4×10^{-17}
Frequency domain (8)	2.468×10^{-15}	2.037×10^{-15}	1.7×10^{-17}

TABLE I: Noise powers.

matches experiments for frequencies below 10 Hz where the flicker noise is dominant and therefore clearly visible.

2) PSD of the RTN: In Fig. 4, $\widehat{S}_{i_d}(f)$ denotes the *estimation* of the actual total drain current noise PSD. It is strongly dominated by the RTN *Lorentzian* [5]:

$$S_{i_{d,RTN}}(f) = \Delta I_D^2 \frac{4\overline{\tau}^2}{\overline{\tau}_e + \overline{\tau}_c} \frac{1}{1 + (2\pi f \overline{\tau})^2} \tag{5}$$

with

$$\overline{\tau} = \frac{1}{\overline{\tau}_c} + \frac{1}{\overline{\tau}_e}. \tag{6}$$

The previously calculated empirical means have been plugged into the model (5). The resulting plateau amplitude and corner frequency are consistent with the ones of $\widehat{S}_{i_d}(f)$, as illustrated in Fig. 4.

3) RTN and $1/f$ Noise Powers: The total drain current noise power is computed as

$$\sigma^2_{i_d} = \frac{1}{T} \int_0^T |i_d(t)|^2 \,\mathrm{d}t, \tag{7}$$

and similarly for extracted $i_{d,RTN}(t)$ and $i_{d,flicker}(t)$. These three noise powers can also be computed by integrating the respective PSD over the measurement bandwidth

$$\sigma^2_{i_d} = \int_{1\,\mathrm{Hz}}^{10^6\,\mathrm{Hz}} S_{i_d}(f)\,\mathrm{d}f. \tag{8}$$

The power of $i_d(t)$ has been computed, using either approaches (7) or (8), after set-up effects have been removed from the signal. For both RTN and flicker noise, (8) is evaluated for the extracted models (5) and (4), respectively. The results are summarized in Table I.

The $1/f$ noise power is overestimated with (7) due to the presence of set-up related and signal processing noise in the trace of Fig. 1c. For the RTN, the relative difference between the two approaches remains below 10 %. In terms of noise powers, the major result is that, although the $1/f$ noise contributes to less than 1 % of the total noise power, here dominated by the RTN, our method allows to extract it from the time-domain measurements.

IV. Conclusion

A rigourous signal-processing methodology aiming at studying the RTN and the flicker noise separately was developed and illustrated for a RTN as strong as $\Delta I_D/I_D \approx 30\,\%$ on a short nMOSFET in weak inversion and saturation. The noise added on top of RTN traces was soundly related to the $1/f$ noise although some background noise still needs to be eliminated. Our methodology was demonstrated to be able to retrieve the $1/f$ component from measured $i_d(t)$ traces even though its PSD and noise power lie two orders of magnitude below the dominant RTN. Power analysis reveals to be a promising approach to quantitatively assess, model and simulate the exact impact of LFN on oscillators, amplifiers and ultra-low power circuits.

Acknowledgements

Léopold Van Brandt is with Université catholique de Louvain as research fellow from the National Foundation for Scientific Research (FNRS) of Belgium through a FRIA grant. The work has been partially funded by French Community of Belgium via ARC NANOSEC project.

References

[1] E. G. Ioannidis, S. Haendler, A. Bajolet, T. Pahron, N. Planes, F. Arnaud, R. A. Bianchi, M. Haond, D. Golanski, J. Rosa, C. Fenouillet-Beranger, P. Perreau, C. A. Dimitriadis, and G. Ghibaudo, “Low frequency noise variability in high-k/metal gate stack 28nm bulk and fd-soi cmos transistors,” in *2011 International Electron Devices Meeting*, Dec 2011, pp. 18.6.1–18.6.4.

[2] J. E. Husseini, F. Martinez, M. Valenza, R. Ritzenthaler, F. Lime, B. Iñiguez, O. Faynot, C. L. Royer, and F. Andrieu, “Modeling of low frequency noise in fd soi mosfets,” *Solid-State Electronics*, vol. 90, pp. 116 – 120, 2013, selected papers from EUROSOI 2012.

[3] C. Theodorou, E. Ioannidis, S. Haendler, E. Josse, C. Dimitriadis, and G. Ghibaudo, “Low frequency noise variability in ultra scaled fd-soi n-mosfets: Dependence on gate bias, frequency and temperature,” *Solid-State Electronics*, vol. 117, pp. 88 – 93, 2016.

[4] J. S. Kolhatkar, L. K. J. Vandamme, C. Salm, and H. Wallinga, “Separation of random telegraph signals from 1/f noise in mosfets under constant and switched bias conditions,” in *ESSDERC ’03. 33rd Conference on European Solid-State Device Research, 2003.*, Sep. 2003, pp. 549–552.

[5] M. Kirton and M. Uren, “Noise in solid-state microstructures: A new perspective on individual defects, interface states and low-frequency (1/f) noise,” *Advances in Physics*, vol. 38, no. 4, pp. 367–468, 1989. [Online]. Available: https://doi.org/10.1080/00018738900101122

[6] C. Marquez, N. Rodriguez, F. Gamiz, R. Ruiz, and A. Ohata, “Electrical characterization of random telegraph noise in fully-depleted silicon-on-insulator mosfets under extended temperature range and back-bias operation,” *Solid-State Electronics*, vol. 117, pp. 60 – 65, 2016.

[7] *E4727A Advanced Low-Frequency Noise Analyzer*, Keysight Technologies, 2018. [Online]. Available: https://literature.cdn.keysight.com/litweb/pdf/5991-4280EN.pdf?id=2462666

[8] A. Papoulis, *Probability, Random Variables, and Stochastic Processes*, ser. McGraw-Hill Series in Electrical Engineering. McGraw-Hill, 1991.

[9] P. Stoica and R. L. Moses, *Spectral analysis of signals.* Pearson Prentice Hall Upper Saddle River, NJ, 2005.